

Open *sd*-shell nuclei from first principles*

G. R. Jansen,^{1,2} M. D. Schuster,¹ A. Signoracci,^{2,3} G. Hagen,^{2,3} and P. Navrátil⁴

¹National Center for Computational Sciences, Oak Ridge National Laboratory, Oak Ridge, TN 37831, USA

²Physics Division, Oak Ridge National Laboratory, Oak Ridge, TN 37831, USA

³Department of Physics and Astronomy, University of Tennessee, Knoxville, TN 37996, USA

⁴TRIUMF, 4004 Wesbrook Mall, Vancouver, British Columbia, V6T 2A3 Canada

We extend the *ab initio* coupled-cluster effective interaction (CCEI) method to open-shell nuclei with protons and neutrons in the valence space, and compute binding energies and excited states of isotopes of neon and magnesium. We employ a nucleon-nucleon and three-nucleon interaction from chiral effective field theory evolved to a lower cutoff via a similarity renormalization group transformation. We find good agreement with experiment for binding energies and spectra, while charge radii of neon isotopes are underestimated. For the deformed nuclei ^{20}Ne and ^{24}Mg we reproduce rotational bands and electric quadrupole transitions within uncertainties estimated from an effective field theory for deformed nuclei, thereby demonstrating that collective phenomena in *sd*-shell nuclei emerge from complex *ab initio* calculations.

Introduction – Nuclei are complex many-body systems that present us with a wealth of interesting quantum mechanical phenomena that emerge along the entire chart of nuclei. These phenomena involve: exotic clustering behavior and extended density distributions of loosely bound nuclei [1, 2], melting and re-organization of shell-structure in neutron nuclei [3–5], Borromean nuclei [6, 7], and emergence of collective behavior in nuclei, such as rotational and vibrational states [8, 9] as well as nuclear super conductivity and pairing [10].

Recently there has been an explosion of nuclear many-body methods with a sufficiently soft computational scaling to allow a reliable description of binding energies and spectra in nuclei up through the *sd*-shell starting from nucleon-nucleon and three-nucleon forces from chiral effective field theory (EFT) [11–16]. In spite of this progress, emergence of collective phenomena in nuclei still poses significant challenges to *ab initio* methods. Rotational states in *p*-shell nuclei have been successfully computed in the no-core shell-model and in Green’s-function Monte-Carlo approaches [17–21], while in the *sd*-shell, deformed nuclei have only been accurately described in shell-model calculations using phenomenological interactions [22]. A symplectic approach has been proposed [23] to enable extension of the no-core shell-model to larger model spaces and higher-mass nuclei, yet prototypical deformed nuclei like ^{20}Ne and ^{48}Cr remain out of reach in the aforementioned approaches. Furthermore, as deformed nuclei are truly open-shell, they

are inaccessible via the typical implementation of many-body expansion methods like coupled cluster theory [24], self-consistent Green’s function methods [25], and in-medium similarity renormalization group (SRG) methods [26], that normally rely on a spherical, closed-shell mean field. Extensions to open-shell nuclei via Bogoliubov coupled cluster theory [27], Gorkov-Green’s function methods [28], and multi-reference in-medium similarity renormalization group methods [14] are underway, but are limited to semi magic nuclei thus far.

Recently, non-perturbative effective interactions for the shell-model were derived from coupled-cluster theory and in-medium SRG starting from chiral nucleon-nucleon and three-nucleon forces [29, 30]. The CCEI approach is based on the valence-cluster expansion of the Hamiltonian that was first proposed within the framework of the no-core shell-model [31], and applied to *p*-shell nuclei [32, 33]. More recently the no-core shell-model was used to construct non-perturbative shell-model interactions for light fluorine isotopes based on nucleon-nucleon interactions only [34].

In this work we extend the CCEI method to deformed nuclei in the *sd*-shell with both protons and neutrons in the valence space. Furthermore, we show that other observables such as charge radii can be consistently computed within CCEI. Diagonalization of the resulting interactions yields the fully-correlated wavefunction in the reduced model space, which is sufficient to describe the properties of deformed nuclei [35]. This enables the description and identification of rotational bands, which we compare with predictions from an EFT developed for deformed nuclei [36–38].

Theory – To minimize spurious center-of-mass motion [39], our coupled-cluster calculations start from the intrinsic, *A*-dependent Hamiltonian,

$$\hat{H} = \sum_{i<j} \left(\frac{(\mathbf{p}_i - \mathbf{p}_j)^2}{2mA} + \hat{V}_{NN}^{(i,j)} \right) + \sum_{i<j<k} \hat{V}_{3N}^{(i,j,k)}. \quad (1)$$

We utilize the same Hamiltonian as in our prior work, [30], with an initial next-to-next-to-next-to lead-

* This manuscript has been authored by UT-Battelle, LLC under Contract No. DE-AC05-00OR22725 with the U.S. Department of Energy. The United States Government retains and the publisher, by accepting the article for publication, acknowledges that the United States Government retains a non-exclusive, paid-up, irrevocable, world-wide license to publish or reproduce the published form of this manuscript, or allow others to do so, for United States Government purposes. The Department of Energy will provide public access to these results of federally sponsored research in accordance with the DOE Public Access Plan. (<http://energy.gov/downloads/doe-public-access-plan>).

ing order two-body chiral interaction and a next-to-next-to leading order three-body chiral interaction, evolved consistently to a lower momentum scale via a similarity renormalization group transformation. This interaction has been demonstrated to yield accurate binding energies and spectra in and around isotopes of oxygen [29, 30, 40, 41]. Here we explore how this Hamiltonian performs in isotopes of neon and magnesium. We perform coupled-cluster calculations in thirteen major oscillator shells with the frequency $\hbar\omega = 20$ MeV, and utilize the normal-ordered two-body approximation for the three-nucleon force with the additional three-body energy cut $E_{3\max} = N_1 + N_2 + N_3 \leq 12$, where N_i refers to the major oscillator shell of the i^{th} particle (see Ref. [30] for more details). In addition, we derive the coupled-cluster effective interactions (CCEI) based on a core of mass A_c , by expanding the Hamiltonian Eq. (1) in a form suitable for the shell model (i.e. the valence-cluster expansion [33]),

$$H_{\text{CCEI}} = H_0^{A_c} + H_1^{A_c+1} + H_2^{A_c+2} + \dots, \quad (2)$$

i.e. for the core, one-body, two-body, and higher body valence-cluster Hamiltonians. As pointed out in Ref. [34] the valence-cluster expansion is not uniquely defined as one can either choose to set the mass A that appears in intrinsic kinetic energy of the individual parts equal to the mass A of the target nucleus, or set it equal to the mass A of the core, one-body, two-body, and higher body parts. Both choices will reproduce the exact result in the limit of including all terms in the valence-cluster expansion. While in Ref. [30] we made the former choice, in this work we choose the latter as defined by Eq. (2) and truncate the cluster expansion at the two-body level. This choice tremendously simplifies the calculations since we can use the same effective shell-model interaction for all nuclei, furthermore this choice guarantees that the Hamiltonians for A_c , A_{c+1} , and A_{c+2} are translationally invariant (see Supplemental Material for a quantitative comparison between these two choices in computing excited states and binding energies in oxygen isotopes). In this work we compute the ground state of the A_c nucleus using the coupled-cluster method in the singles-and-doubles approximation with the Λ -triples correction treated perturbatively (Λ -CCSD(T)) [42, 43], while the one- and two-particle-attached equation-of-motion coupled-cluster (EOM-CC) methods are used to compute the ground and excited states of the $A_c + 1$ and $A_c + 2$ nuclei [44–47]. In this work we define our valence space by the sd -shell, and we use the Okubo-Lee-Suzuki similarity transformation [48–50] to project the one- and two-particle-attached EOM-CC eigenstates with the largest overlap with the model space onto two-body valence-space states. From the non-Hermitian coupled-cluster procedure, one can obtain a Hermitian effective Hamiltonian for use in standard shell model codes by constructing the metric operator $S^\dagger S$ where S is a matrix that diagonalizes H_{CCEI}^A ; the Hermitian shell-model Hamiltonian is then $[S^\dagger S]^{1/2} H_{\text{CCEI}}^A [S^\dagger S]^{-1/2}$ [51, 52].

Any operator O can be expanded in a similar form to Eq. (2), suitable for the shell model (see Refs. [32, 53] for details), $O_{\text{CCEI}} = O_0^{A_c} + O_1^{A_c+1} + O_2^{A_c+2} + \dots$, with a consistent (i.e. identical to that of the Hamiltonian) Okubo-Lee-Suzuki transformation and metric operator. In this way, any operator which can be computed for all many-body states in the $A_c, A_c + 1, A_c + 2$ systems in coupled-cluster theory can be used to define a valence-space operator.

Results – As we in this work adopt a different definition for the valence-cluster expansion as used in Ref. [30], we would first like to address the accuracy of our calculations. Again, we find good agreement between full-space CC and CCEI for binding energies in the oxygen isotopes, and for low-lying excited states in $^{22,24}\text{O}$. In particular, for ^{22}O CCEI yields a $J^\pi = 2^+$ excited state at 2.6 MeV and a $J^\pi = 3^+$ excited state at 3.8 MeV, while full-space EOM-CC with singles and doubles excitations (EOM-CCSD) yields the corresponding excited states at 2.5 MeV and 3.8 MeV, respectively. For the $J^\pi = 2^+$ and $J^\pi = 1^+$ excited states in ^{24}O CCEI gives 5.7 MeV and 6.4 MeV, while EOM-CCSD yields 6.0 MeV and 6.4 MeV, respectively. The CCEI results for the binding energies of $^{22,24}\text{O}$ are 162.2 MeV and 168.1 MeV, while the corresponding full-space Λ -CCSD(T) results are 162.0 MeV and 170.2 MeV, respectively. We refer the reader to the Supplemental Material for a more detailed comparison between full-space coupled-cluster calculations and results obtained using the A -dependent and A -independent choices in the CCEI method.

In this work we extend the CCEI approach to nuclei with protons and neutrons in the valence space, and to gauge the accuracy of CCEI for these systems we benchmark against the full-space charge-exchange EOM-CC method [54] for ground- and excited states in ^{24}F and ^{24}Ne . To obtain a more precise calculation of ^{24}Ne as a double charge-exchange excitation from the ground-state of ^{24}O , we extend the charge-exchange EOM-CC method beyond the two-particle-two-hole excitation level (EOM-CCSD), and include the leading-order three-particle-three-hole ($3p$ - $3h$) excitations defined by the EOM-CCSDT-1 method [55]. Since this approach is rather costly in terms of computational cycles and memory, we introduce an active-space [56] truncation on the allowed $3p$ - $3h$ excitations in the unoccupied space defined by an energy cut $e_{3\max} = N_1 + N_2 + N_3$ (similar to the $E_{3\max}$ cut of the three-nucleon force). This approach allows us to compute ground- and excited states of nuclei that differ by two units of the z -component of the total isospin (double charge-exchange) from the closed (sub-)shell reference nucleus, and here we present the first application of this method to ground and excited states of ^{24}Ne . Figure 1 shows the low-lying spectra of ^{24}F and ^{24}Ne computed with full-space (double) charge-exchange EOM-CCSD and EOM-CCSDT-1 and CCEI, including a comparison to data. The agreement between the CCEI and full-space charge-exchange EOM-CCSDT-1 for ^{24}F is overall good, and we see that the effect of including

$3p$ - $3h$ excitations is rather small on most of the computed excitation levels (except for the second 1^+ excited state that moves down by about 0.5 MeV). For ^{24}Ne the agreement between EOM-CCSDT-1 and CCEI is overall satisfactory. In particular the first 0^+ state is in excellent agreement, and the role of $3p$ - $3h$ excitations is small. For the first 2^+ and 4^+ states we see that $3p$ - $3h$ are more important and brings the EOM-CCSDT-1 result in closer agreement with CCEI. The agreement with data for ^{24}F and ^{24}Ne is also quite good. For ^{24}F both CCEI and full-space coupled-cluster yield a ground-state with spin and parity $J^\pi = 3^+$ in agreement with experiment [57]. Finally, we also compared our results to those computed with in-medium SRG effective interactions and the recent measurements of excited states in ^{24}F [57], and found good agreement.

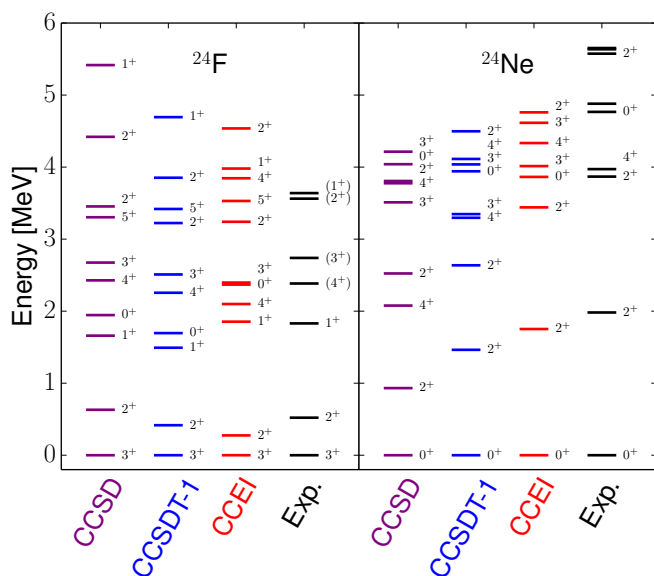


FIG. 1. (Color online) Excited states of ^{24}F (left panel) and ^{24}Ne (right panel) computed from the charge-exchange EOM-CCSD, EOM-CCSDT-1, CCEI, and compared to data.

For the binding energies of ^{24}F and ^{24}Ne we obtain 179.4 MeV and 192.9 MeV in CCEI, respectively, in good agreement with the full-space coupled-cluster results of 181.0 MeV and 190.8 MeV, respectively. Both CCEI and full-space coupled-cluster results are in good agreement with the experimental binding energies of 179.9 MeV and 191.8 MeV [58]. Finally we checked that our calculations are reasonably well converged with respect to the model-space size. In our full-space charge-exchange EOM-CCSDT-1 calculations we used $N_{\text{max}} = 12$ and an active space of $e_{3\text{max}} = 12$ for the $3p$ - $3h$ excitations for the ground- and excited states in ^{24}F , while for the excited states in ^{24}Ne we used $e_{3\text{max}} = 14$, and finally for the ground-state of ^{24}Ne we used $e_{3\text{max}} = 20$. We found that energies are converged to within a few hundred keV with respect to these active-space truncations. Beyond the active space truncation, there are also uncertainties

associated with the truncation of the particle-hole excitation level in the EOM-CC approaches used to compute the full-space charge exchange excitations (see Fig. 1), and in the construction of the core-, one-body, and two-body parts of the CCEI defined in Eq. (2). We refer the reader to [30] for a more detailed discussion on uncertainties related to the construction of CCEI and the model-space truncations used.

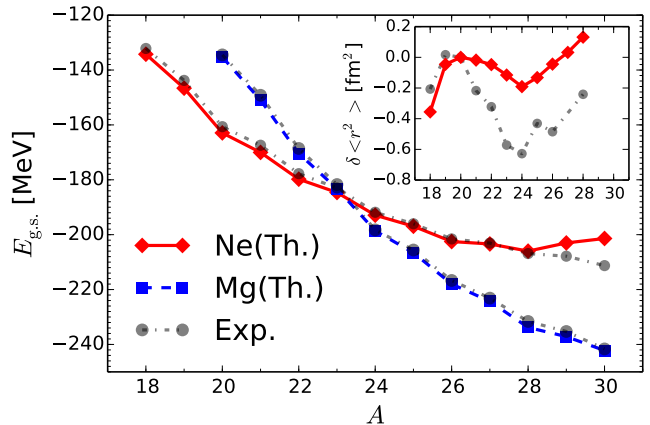


FIG. 2. (Color online) Ground-state energies of neon (red line marked with diamonds) and magnesium isotopes (blue line marked with squares). Gray dashed-dotted lines marked with circles show the experimental values. The inset shows the CCEI results for the isotope shifts in neon isotopes, relative to ^{20}Ne , compared to known experimental data.

Figure 2 shows the total binding energies for $^{18-30}\text{Ne}$ and $^{20-30}\text{Mg}$ obtained from our CCEI calculations and are compared to data. We find a very good agreement between the CCEI results and experiment for all magnesium isotopes and for neon isotopes up to mass $A = 28$. The deviation between the CCEI results and experiment for $^{29,30}\text{Ne}$ is not unexpected as these nuclei are part of the well-known island of inversion region [59], for which intruder states from the fp -shell become important. We also computed binding energies for all isotope chains in the sd -shell and found overall very good agreement with data (see Supplement Material). In the inset, we show the computed isotope shifts of the charge radii for the neon isotopes for which experimental data is available [60]. The CCEI calculations included the core and one-body contributions to the radii, while the more demanding inclusion of two-body contributions will be explored in the future. The overall trend, in particular the kink at $N = 24$, is reproduced qualitatively.

In Fig. 3, we highlight the level schemes of a subset of the computed neon and magnesium isotopes, including the prototypical deformed nuclei ^{20}Ne and ^{24}Mg , as well as odd- A and neutron-rich exotic nuclei like ^{27}Ne , for which little experimental data is known. We observe a quite reasonable reproduction of the data in all cases, with a generally consistent compression of the level scheme. We also observe rotational band structures in

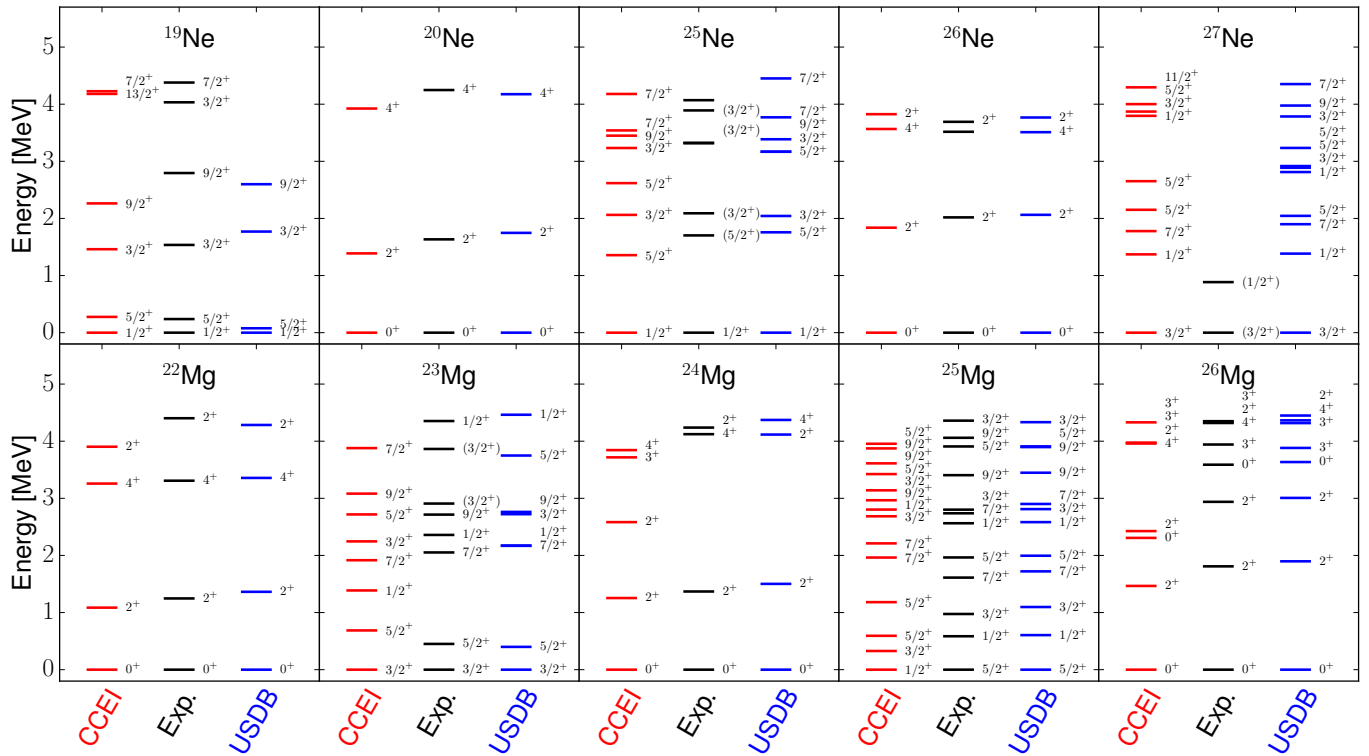


FIG. 3. (Color online) Excitation spectra of selected neon (upper panel) and magnesium (lower panel) isotopes. The left columns (red lines) display the CCEI results, the middle columns (black lines) include known positive-parity experimental states from the ENSDF database, while the right columns (blue lines) shows excitation spectra obtained from the USDB interaction [35].

these isotopic chains, as suggested from experimental studies.

The quality of these level schemes can be difficult to measure with respect to experiment. To address the agreement with data and to compare with the phenomenological USD-B interaction in a more quantitative way we perform a comparison of the root-mean-squared (rms) deviations obtained from 144 experimental levels in the lower sd-shell. For the CCEI (USDB) shell-model interactions, we find values of 591(244) keV for oxygen, 452(268) keV in fluorine, 422(268) keV in neon, 529(155) keV in sodium and 760(106) keV magnesium. We note that the CCEI rms deviations are very close to the corresponding IM-SRG rms deviations reported in Stroberg et al. [61].

Let us now turn to the deformed nuclei ^{20}Ne and ^{24}Mg in more detail. Deformed even-even nuclei exhibit ground-state rotational bands with energies $E(I) = \alpha_0 I(I+1)[1 + \alpha_2 I(I+1) + \dots]$ [8, 9, 62]. Here, $I = 0, 2, 4, \dots$ denotes the spin, α_0 is the rotational constant (i.e. twice the inverse of the moment of inertia), and $\alpha_2 \ll 1$ is a small correction. Similarly, strengths of electric quadrupole transitions $B(E2 \downarrow, I_i) = Q_0^2 (\text{CG})^2 [1 + \beta_2 I_i(I_i - 1) + \dots]$ from an initial spin I_i to final spin $I_i - 2$ can be expanded as a function of spin [63, 64]. Here CG denotes a Clebsch Gordan coefficient that ac-

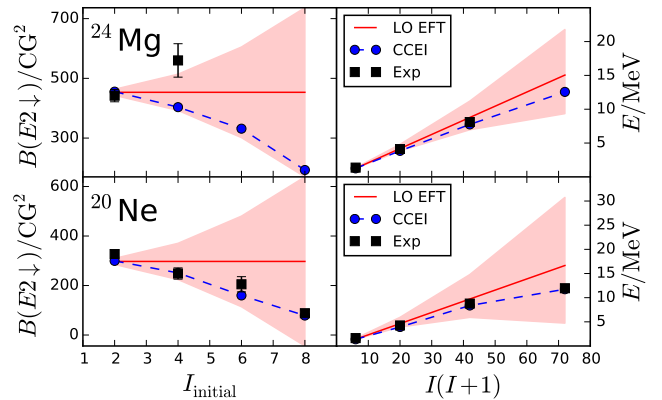


FIG. 4. (Color online) $B(E2 \downarrow)$ transition strengths, divided by a squared Clebsch Gordan coefficient CG, as a function of initial spin (left panels) and corresponding excitation energies as a function of spin (right panels) for ^{24}Mg (top panels) and ^{20}Ne (bottom panels). Data (black squares) and results from CCEI (blue circles connected by dashed lines) are shown together with results from a leading-order EFT for deformed nuclei (red line and shaded uncertainty estimates).

counts for geometric aspects in the transition, while Q_0 and $\beta_2 \ll 1$ are low-energy constants. For a rigid rotor,

$\alpha_2 = 0 = \beta_2$. The relations for energies and $B(E2)$ transitions, well known from collective models of the atomic nucleus [65–67], were recently re-derived via EFT [36–38]. The EFT exploits the separation of scale between the energy ξ of rotations and the breakdown energy Ω that marks the proliferation of non-rotational degrees of freedom. For even-even sd -shell nuclei $\xi \approx 1.5$ MeV, and $\Omega \approx 6$ MeV. The low-energy constants α_2 and β_2 that account for deviations from the rigid rotor are of the order $(\xi/\Omega)^2$. Figure 4 shows that computed $B(E2)$ transitions and spectra agree well with data for ^{20}Ne and ^{24}Mg . Note that for $B(E2)$ we used the standard effective charges of $e_{\text{eff}}^p = 1.5e$ and $e_{\text{eff}}^n = 0.5e$, for protons and neutrons, respectively. We verified that the results shown for the $B(E2)$ transitions are not sensitive to small variations of the effective charge. Furthermore, in Navrátil et al. [32] it was shown that these phenomenological effective charges are close to fully microscopically derived effective charges for the p -shell. In agreement with EFT results, the deviations from the rigid-rotor behavior (red solid lines) are of similar size for spectra and transitions, and within EFT uncertainty estimates (red shaded regions).

Conclusions – In this work we extended the *ab initio* CCEI method to deformed sd -shell nuclei. We presented results for binding energies and excited states in isotopes of neon and magnesium based on chiral nucleon-nucleon and three-nucleon forces. The results were found to be in good agreement with data. Our calculations reproduce rotational bands and $B(E2)$ transitions in ^{20}Ne and ^{24}Mg within the uncertainties estimated from an EFT derived for deformed nuclei. We have thus extended the description of collective degrees of freedom as emergent phenomena in sd -shell nuclei from first principles. This work

paves the way for non-perturbative shell-model Hamiltonians tied to chiral EFT, with predictive power in the sd -shell and beyond.

ACKNOWLEDGMENTS

We would in particular like to thank Ragnar Stroberg for computing the rms deviations from experiment for our CCEI results and for providing us with shell-model results for the sd -shell nuclei considered in this work using the USD-B interaction. We also thank Heiko Hergert, Jason Holt, Jonathan Engel and Thomas Papenbrock for useful discussions. We are particularly grateful to Thomas Papenbrock for generating Figure 4 and contributing to the discussion related to the effective field theory for deformed nuclei. This work was supported by the Office of Nuclear Physics, U.S. Department of Energy (Oak Ridge National Laboratory), de-sc0008499 (NUCLEI SciDAC collaboration), NERRSC Grant No. 491045-2011, and the Field Work Proposal ERKBP57 at Oak Ridge National Laboratory. Computer time was provided by the Innovative and Novel Computational Impact on Theory and Experiment (INCITE) program. TRIUMF receives funding via a contribution through the National Research Council Canada. This research used resources of the Oak Ridge Leadership Computing Facility located in the Oak Ridge National Laboratory, which is supported by the Office of Science of the Department of Energy under Contract No. DE-AC05-00OR22725, and used computational resources of the National Center for Computational Sciences and the National Institute for Computational Sciences.

-
- [1] E. Epelbaum, H. Krebs, D. Lee, and U.-G. Meißner, Phys. Rev. Lett. **106**, 192501 (2011), URL <http://link.aps.org/doi/10.1103/PhysRevLett.106.192501>.
- [2] I. Tanihata, H. Savajols, and R. Kanungo, Prog. Part. Nucl. Phys. **68**, 215 (2013), URL <http://www.sciencedirect.com/science/article/pii/S0146641012001081>.
- [3] G. Hagen, M. Hjorth-Jensen, G. R. Jansen, R. Machleidt, and T. Papenbrock, Phys. Rev. Lett. **109**, 032502 (2012), URL <http://link.aps.org/doi/10.1103/PhysRevLett.109.032502>.
- [4] J. D. Holt, T. Otsuka, A. Schwenk, and T. Suzuki, Journal of Physics G: Nuclear and Particle Physics **39**, 085111 (2012), URL <http://stacks.iop.org/0954-3899/39/i=8/a=085111>.
- [5] D. Steppenbeck, S. Takeuchi, N. Aoi, P. Doornenbal, J. Lee, M. Matsushita, H. Wang, H. Baba, N. Fukuda, S. Go, et al., Journal of Physics: Conference Series **445**, 012012 (2013), URL <http://stacks.iop.org/1742-6596/445/i=1/a=012012>.
- [6] I. Tanihata, H. Hamagaki, O. Hashimoto, Y. Shida, N. Yoshikawa, K. Sugimoto, O. Yamakawa, T. Kobayashi, and N. Takahashi, Phys. Rev. Lett. **55**, 2676 (1985), URL <http://link.aps.org/doi/10.1103/PhysRevLett.55.2676>.
- [7] M. Zhukov, B. Danilin, D. Fedorov, J. Bang, I. Thompson, and J. Vaagen, Physics Reports **231**, 151 (1993), ISSN 0370-1573, URL <http://www.sciencedirect.com/science/article/pii/037015739390141Y>.
- [8] A. Bohr, Dan. Mat. Fys. Medd. **26**, no. 14 (1952).
- [9] A. Bohr and B. R. Mottelson, Dan. Mat. Fys. Medd. **27**, no. 16 (1953).
- [10] A. Bohr, B. R. Mottelson, and D. Pines, Phys. Rev. **110**, 936 (1958), URL <http://link.aps.org/doi/10.1103/PhysRev.110.936>.
- [11] K. Hebeler, J. Holt, J. Menendez, and A. Schwenk, Annual Review of Nuclear and Particle Science **65**, null (2015), <http://dx.doi.org/10.1146/annurev-nucl-102313-025446>, URL <http://dx.doi.org/10.1146/annurev-nucl-102313-025446>.
- [12] J. Simonis, K. Hebeler, J. D. Holt, J. Menendez, and A. Schwenk, ArXiv e-prints (2015), 1508.05040, URL <http://adsabs.harvard.edu/abs/2015arXiv150805040S>.
- [13] S. Binder, J. Langhammer, A. Calci, and R. Roth, Phys. Lett. B **736**, 119 (2014), URL

- <http://www.sciencedirect.com/science/article/pii/S0370269314004961>.
- [14] H. Hergert, S. K. Bogner, T. D. Morris, S. Binder, A. Calci, J. Langhammer, and R. Roth, *Phys. Rev. C* **90**, 041302 (2014), URL <http://link.aps.org/doi/10.1103/PhysRevC.90.041302>.
- [15] A. Ekström, G. R. Jansen, K. A. Wendt, G. Hagen, T. Papenbrock, B. D. Carlsson, C. Forssén, M. Hjorth-Jensen, P. Navrátil, and W. Nazarewicz, *Phys. Rev. C* **91**, 051301 (2015), URL <http://link.aps.org/doi/10.1103/PhysRevC.91.051301>.
- [16] G. Hagen, A. Ekström, C. Forssén, G. R. Jansen, W. Nazarewicz, T. Papenbrock, K. A. Wendt, S. Bacca, N. Barnea, B. Carlsson, et al., *Nature Physics* **advance online publication** (2015), URL <http://www.nature.com/nphys/journal/vaop/ncurrent/pdf/nphys3529.pdf>.
- [17] E. Caurier, P. Navrátil, W. E. Ormand, and J. P. Vary, *Phys. Rev. C* **64**, 051301 (2001), URL <http://link.aps.org/doi/10.1103/PhysRevC.64.051301>.
- [18] S. C. Pieper, R. B. Wiringa, and J. Carlson, *Phys. Rev. C* **70**, 054325 (2004), URL <http://link.aps.org/doi/10.1103/PhysRevC.70.054325>.
- [19] M. A. Caprio, P. Maris, J. P. Vary, and R. Smith, *ArXiv e-prints* (2015), 1509.00102.
- [20] M. A. Caprio, P. Maris, J. P. Vary, and R. Smith, *International Journal of Modern Physics E* **0**, 1541002 (0), URL <http://www.worldscientific.com/doi/abs/10.1142/S0218301315410025>.
- [21] P. Maris, M. A. Caprio, and J. P. Vary, *Phys. Rev. C* **91**, 014310 (2015), URL <http://link.aps.org/doi/10.1103/PhysRevC.91.014310>.
- [22] E. Caurier, G. Martínez-Pinedo, F. Nowacki, A. Poves, and A. P. Zuker, *Rev. Mod. Phys.* **77**, 427 (2005), URL <http://link.aps.org/doi/10.1103/RevModPhys.77.427>.
- [23] T. Dytrych, K. D. Launey, J. P. Draayer, P. Maris, J. P. Vary, E. Saule, U. Catalyurek, M. Sosonkina, D. Langr, and M. A. Caprio, *Phys. Rev. Lett.* **111**, 252501 (2013), URL <http://link.aps.org/doi/10.1103/PhysRevLett.111.252501>.
- [24] G. Hagen, T. Papenbrock, M. Hjorth-Jensen, and D. J. Dean, *Reports on Progress in Physics* **77**, 096302 (2014), URL <http://stacks.iop.org/0034-4885/77/i=9/a=096302>.
- [25] W. Dickhoff and C. Barbieri, *Prog. Part. Nucl. Phys.* **52**, 377 (2004), URL <http://www.sciencedirect.com/science/article/pii/S0146641004000535>.
- [26] H. Hergert, S. K. Bogner, S. Binder, A. Calci, J. Langhammer, R. Roth, and A. Schwenk, *Phys. Rev. C* **87**, 034307 (2013), URL <http://link.aps.org/doi/10.1103/PhysRevC.87.034307>.
- [27] A. Signoracci, T. Duguet, G. Hagen, and G. R. Jansen, *Phys. Rev. C* **91**, 064320 (2015), URL <http://link.aps.org/doi/10.1103/PhysRevC.91.064320>.
- [28] V. Somà, C. Barbieri, and T. Duguet, *Phys. Rev. C* **87**, 011303 (2013), URL <http://link.aps.org/doi/10.1103/PhysRevC.87.011303>.
- [29] S. K. Bogner, H. Hergert, J. D. Holt, A. Schwenk, S. Binder, A. Calci, J. Langhammer, and R. Roth, *Phys. Rev. Lett.* **113**, 142501 (2014), URL <http://link.aps.org/doi/10.1103/PhysRevLett.113.142501>.
- [30] G. R. Jansen, J. Engel, G. Hagen, P. Navrátil, and A. Signoracci, *Phys. Rev. Lett.* **113**, 142502 (2014), URL <http://link.aps.org/doi/10.1103/PhysRevLett.113.142502>.
- [31] B. R. Barrett, P. Navrátil, and J. P. Vary, *Prog. Part. Nucl. Phys.* **69**, 131 (2013), URL <http://www.sciencedirect.com/science/article/pii/S0146641012001184>.
- [32] P. Navrátil, M. Thoresen, and B. R. Barrett, *Phys. Rev. C* **55**, R573 (1997), URL <http://link.aps.org/doi/10.1103/PhysRevC.55.R573>.
- [33] A. F. Lisetskiy, B. R. Barrett, M. K. G. Kruse, P. Navrátil, I. Stetcu, and J. P. Vary, *Phys. Rev. C* **78**, 044302 (2008), URL <http://link.aps.org/doi/10.1103/PhysRevC.78.044302>.
- [34] E. Dikmen, A. F. Lisetskiy, B. R. Barrett, P. Maris, A. M. Shirokov, and J. P. Vary, *Phys. Rev. C* **91**, 064301 (2015), URL <http://link.aps.org/doi/10.1103/PhysRevC.91.064301>.
- [35] B. A. Brown and W. A. Richter, *Physical Review C (Nuclear Physics)* **74**, 034315 (pages 11) (2006), URL <http://link.aps.org/abstract/PRC/v74/e034315>.
- [36] T. Papenbrock, *Nuclear Physics A* **852**, 36 (2011), URL <http://www.sciencedirect.com/science/article/pii/S0375947410007773>.
- [37] T. Papenbrock and H. A. Weidenmüller, *Phys. Rev. C* **89**, 014334 (2014), URL <http://link.aps.org/doi/10.1103/PhysRevC.89.014334>.
- [38] E. A. Coello Pérez and T. Papenbrock, *Phys. Rev. C* **92**, 014323 (2015), URL <http://link.aps.org/doi/10.1103/PhysRevC.92.014323>.
- [39] G. Hagen, T. Papenbrock, and D. J. Dean, *Phys. Rev. Lett.* **103**, 062503 (2009), URL <http://link.aps.org/doi/10.1103/PhysRevLett.103.062503>.
- [40] H. Hergert, S. Binder, A. Calci, J. Langhammer, and R. Roth, *Phys. Rev. Lett.* **110**, 242501 (2013), URL <http://link.aps.org/doi/10.1103/PhysRevLett.110.242501>.
- [41] A. Cipollone, C. Barbieri, and P. Navrátil, *Phys. Rev. Lett.* **111**, 062501 (2013), URL <http://link.aps.org/doi/10.1103/PhysRevLett.111.062501>.
- [42] A. G. Taube and R. J. Bartlett, *J. Chem. Phys.* **128**, 044110 (pages 13) (2008), URL <http://link.aip.org/link/?JCP/128/044110/1>.
- [43] G. Hagen, T. Papenbrock, D. J. Dean, and M. Hjorth-Jensen, *Phys. Rev. C* **82**, 034330 (2010), URL <http://link.aps.org/doi/10.1103/PhysRevC.82.034330>.
- [44] J. R. Gour, P. Piecuch, M. Hjorth-Jensen, M. Włoch, and D. J. Dean, *Phys. Rev. C* **74**, 024310 (2006), URL <http://link.aps.org/doi/10.1103/PhysRevC.74.024310>.
- [45] G. R. Jansen, M. Hjorth-Jensen, G. Hagen, and T. Papenbrock, *Phys. Rev. C* **83**, 054306 (2011), URL <http://link.aps.org/doi/10.1103/PhysRevC.83.054306>.
- [46] G. R. Jansen, *Phys. Rev. C* **88**, 024305 (2013), URL <http://link.aps.org/doi/10.1103/PhysRevC.88.024305>.
- [47] J. Shen and P. Piecuch, *Molecular Physics* **112**, 868 (2014), URL <http://dx.doi.org/10.1080/00268976.2014.886397>.
- [48] S. Okubo, *Progress of Theoretical Physics* **12**, 603 (1954), <http://ptp.oxfordjournals.org/content/12/5/603.full.pdf+html>, URL <http://ptp.oxfordjournals.org/content/12/5/603.abstract>.
- [49] K. Suzuki, *Progress of Theoretical Physics* **68**, 246 (1982), URL <http://ptp.oxfordjournals.org/content/68/1/246.abstract>.

- [50] S. Kvaal, Phys. Rev. C **78**, 044330 (2008), URL <http://link.aps.org/doi/10.1103/PhysRevC.78.044330>.
- [51] F. Scholtz, H. Geyer, and F. Hahne, Annals of Physics **213**, 74 (1992), ISSN 0003-4916, URL <http://www.sciencedirect.com/science/article/pii/000349169290284S>.
- [52] P. Navrátil and B. R. Barrett, Phys. Rev. C **54**, 2986 (1996), URL <http://link.aps.org/doi/10.1103/PhysRevC.54.2986>.
- [53] A. F. Lisetskiy, M. K. G. Kruse, B. R. Barrett, P. Navratil, I. Stetcu, and J. P. Vary, Phys. Rev. C **80**, 024315 (2009), URL <http://link.aps.org/doi/10.1103/PhysRevC.80.024315>.
- [54] A. Ekström, G. R. Jansen, K. A. Wendt, G. Hagen, T. Papenbrock, S. Bacca, B. Carlsson, and D. Gazit, ArXiv e-prints (2014), 1406.4696, URL <http://adsabs.harvard.edu/abs/2014arXiv1406.4696E>.
- [55] J. D. Watts and R. J. Bartlett, Chemical Physics Letters **233**, 81 (1995), ISSN 0009-2614, URL <http://www.sciencedirect.com/science/article/pii/000926149401434W>.
- [56] J. R. Gour, P. Piecuch, and M. Woch, The Journal of Chemical Physics **123**, 134113 (2005), URL <http://scitation.aip.org/content/aip/journal/jcp/123/13/10.1063/1.2042452>.
- [57] L. Cáceres, A. Lepailleur, O. Sorlin, M. Stanoiu, D. Sohler, Z. Dombrádi, S. K. Bogner, B. A. Brown, H. Hergert, J. D. Holt, et al., Phys. Rev. C **92**, 014327 (2015), URL <http://link.aps.org/doi/10.1103/PhysRevC.92.014327>.
- [58] M. Wang, G. Audi, A. Wapstra, F. Kondev, M. McCormick, X. Xu, and B. Pfeiffer, Chinese Physics C **36**, 1603 (2012), URL <http://stacks.iop.org/1674-1137/36/i=12/a=003>.
- [59] K. Marinova, W. Geithner, M. Kowalska, K. Blaum, S. Kappertz, M. Keim, S. Kloos, G. Kotrotsios, P. Lievens, R. Neugart, et al., Phys. Rev. C **84**, 034313 (2011), URL <http://link.aps.org/doi/10.1103/PhysRevC.84.034313>.
- [60] I. Angeli and K. Marinova, At. Data Nucl. Data Tables **99**, 69 (2013), URL <http://www.sciencedirect.com/science/article/pii/S0092640X12000265>.
- [61] S. R. Stroberg, H. Hergert, J. D. Holt, S. K. Bogner, and A. Schwenk, Phys. Rev. C **93**, 051301 (2016), URL <http://link.aps.org/doi/10.1103/PhysRevC.93.051301>.
- [62] M. A. J. Mariscotti, G. Scharff-Goldhaber, and B. Buck, Phys. Rev. **178**, 1864 (1969), URL <http://link.aps.org/doi/10.1103/PhysRev.178.1864>.
- [63] M. V. Mikhailov, Izv. Acad. Nauk SSSR, Ser. Fiz. **28**, 308 (1964).
- [64] M. V. Mikhailov, Izv. Acad. Nauk SSSR, Ser. Fiz. **30**, 1392 (1966).
- [65] J. M. Eisenberg and W. Greiner, *Nuclear Models: Collective and Single-Particle Phenomena* (North-Holland Publishing Company Ltd., London, 1970).
- [66] A. Bohr and B. R. Mottelson, *Nuclear Structure*, vol. II: Nuclear Deformation (W. A. Benjamin, Reading, Massachusetts, USA, 1975), ISBN 9780805310160.
- [67] F. Iachello and A. Arima, *The Interacting Boson Model* (Cambridge University Press, Cambridge, UK, 1987).

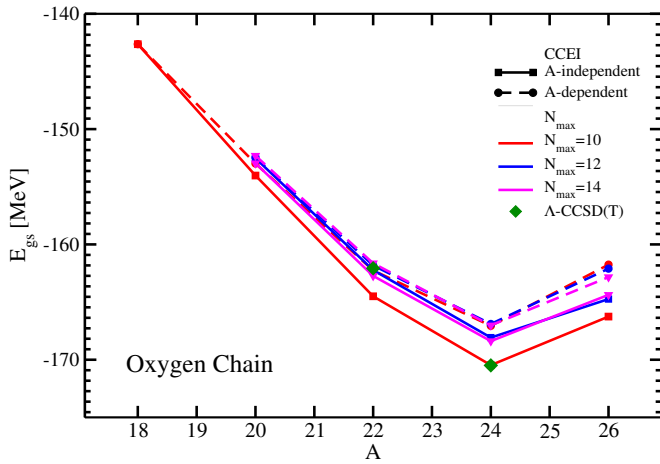


FIG. 1. (Color online) Ground state energies of the oxygen chain using two constructions of the CCEI: A -independent (solid lines) and A -dependent (dashed lines) (see text for description), computed using a coupled cluster model space of $N_{\max} = 10$ (red), 12 (blue) and 14 (magenta) compared to full space Λ -CCSD(T) (diamonds). The calculations were performed using the chiral nucleon-nucleon and three-nucleon interaction used in this work.

Supplementary material. – When constructing the CCEI one can choose the mass A that appears in the intrinsic kinetic energy of the individual parts of the valence cluster expansion in two ways: (i) by the mass of the target nucleus or (ii) by the mass of the core, one-body and two-body parts. This freedom has a relatively large impact on the computation time and, as we will see below, less so on the binding energy and excited states of the target nucleus. Computationally, the former method requires the calculation of the CCEI for each desired A , whereas the latter choice only needs one CCEI calculation which can then be used for any nucleus in the valence space. In Fig. 1 we show the computed CCEI ground-state energies for selected oxygen isotopes using a model-space size of $N_{\max} = 10$, 12, and 14 and the chiral nucleon-nucleon and three-nucleon force used in this work. The CCEI results are then compared to the full-space Λ -CCSD(T) results.

The ground state energy calculations are converged to less than 0.4% with respect to the model-space used to generate the CCEI at $N_{\max} = 14$. The ground-state energies computed using the A -dependent and A -independent CCEI approach converge as the size of the model space is increased. We observe that the A -independent CCEI results track closer to the full-space Λ -CCSD(T) results than the corresponding A -dependent CCEI results. We note that for the results presented in Fig. 1 the full-space coupled-cluster method uses a Hamiltonian that is normal-ordered with respect to the reference states of $^{22,24,28}\text{O}$, respectively. For CCEI method we normal-order the Hamiltonian with respect to ^{16}O . As we are using the normal-ordered two-body approximation and thereby neglect the residual normal-ordered three-body

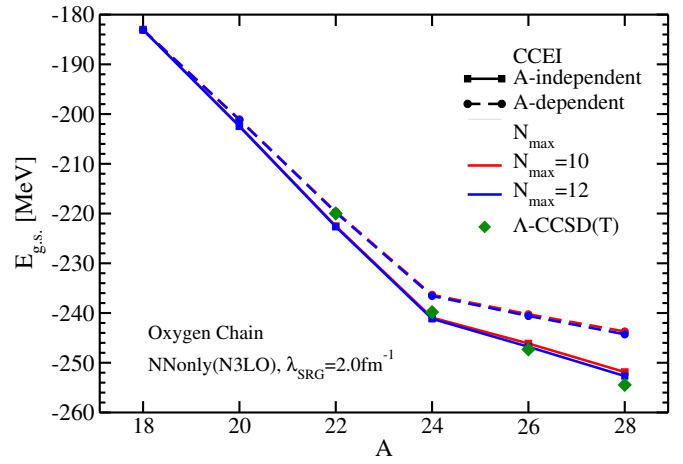


FIG. 2. (Color online) Ground state energies of the oxygen chain using two constructions of the CCEI: A -independent (solid lines) and A -dependent (dashed lines) (see text for description), computed using a coupled cluster model space of $N_{\max} = 10$ (red) and 12 (blue) compared to full space Λ -CCSD(T) (diamonds). The calculations were performed using the chiral nucleon-nucleon interaction N^3LO of [?] evolved via SRG to $\lambda = 2.0\text{fm}^{-1}$.

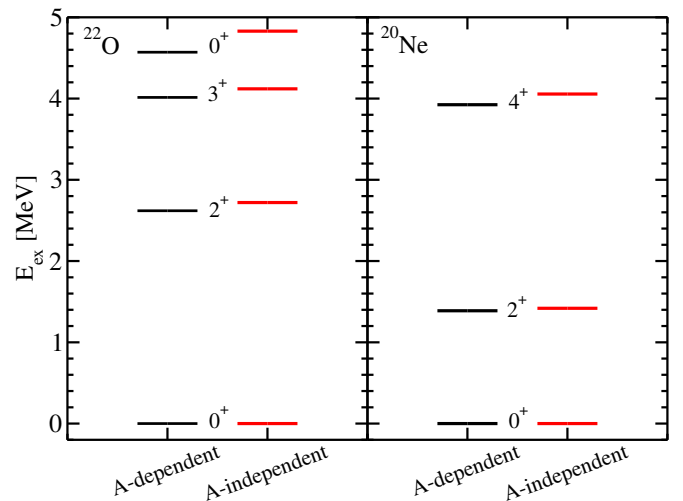


FIG. 3. (Color online) Spectra of ^{22}O (left panel) and ^{20}Ne (right panel) using two constructions of the CCEI: A -independent and A -dependent (see text for description). The calculations were performed using the chiral nucleon-nucleon and three-nucleon interaction used in this work.

parts of the Hamiltonian, one might argue that the full-space coupled-cluster and CCEI results for $^{22,24,28}\text{O}$ are based on slightly different Hamiltonians. In order to remove the effects of the normal ordering with respect to different reference states in our A -dependence investigation of the CCEI, we also computed the oxygen chain using only the nucleon-nucleon interaction of our Hamiltonian, shown in Figure 2.

Here we generate the CCEI using the A -independent and A -dependent constructions at $N_{\max}=10$ and 12 and

compare them to full space Λ -CCSD(T) calculations. The A -independent construction tracks the full space calculations even better than when we include the three-body force. This helps to strengthen our choice in using the A -independent CCEI as our preferred method. Figure 3 shows the spectra of ^{22}O and ^{20}Ne for both the A -independent and A -dependent interactions.

The change in spectra between the two CCEI interactions is generally small, with an average shift of approximately 100 keV. This is comparable to the average shift due to the change in model-space size. The largest shifts tend to appear in the higher lying states, e.g. the approximately 200 keV shift in the second 0^+ state in ^{22}O and the 150 keV shift in the 4^+ state in ^{20}Ne . Since the difference between the two constructions of the CCEI has the largest affect on the binding energies, we choose the A -independent interaction as our preferred method. Not only is it easier from a computational perspective, it also tends to give the best results when compared to full-space coupled-cluster calculations considered here. Figure 4 shows the binding energies for isotope chains in the sd -shell obtained in our CCEI approach and compared to experimental data.

The CCEI shell-model Hamiltonian in the two-body valence-cluster approximation is given by

$$H_{\text{CCEI}} = H_0^{A_c} + H_1^{A_c+1} + H_2^{A_c+2}, \quad (1)$$

here $H_0^{A_c}$ is the the core ground-state energy, $H_1^{A_c+1}$ is the one-body part and $H_2^{A_c+2}$ the two-body part. In this work the ^{16}O core energy computed in the Λ -CCSD(T) approximation is -131.39 MeV. The diagonal one-body matrix elements $\langle a|H_1^{A_c+1}|a\rangle$ for the sd -shell is given in Table I, while the two-body matrix elements $\langle ab|H_2^{A_c+2}|cd\rangle$ are given in Tables II and III.

a	n_a	l_a	$2j_a$	$2t_{z_a}$	$\langle a H_1^{A_c+1} a\rangle$
1	0	2	3	-1	7.05777400
2	0	2	5	-1	-0.25337698
3	1	0	1	-1	1.10565334
4	0	2	3	1	3.85759640
5	0	2	5	1	-3.93783920
6	1	0	1	1	-2.25063950

TABLE I. Single-particle basis and one-body matrix-elements for the sd -shell from CCEI. a labels the single-particle orbit with corresponding quantum numbers $n_a l_a j_a t_{z_a}$ (nodal number, orbital angular momentum, total angular momentum, and isospin projection $t_z = -1/2$ for protons and $t_z = 1/2$ for neutrons).

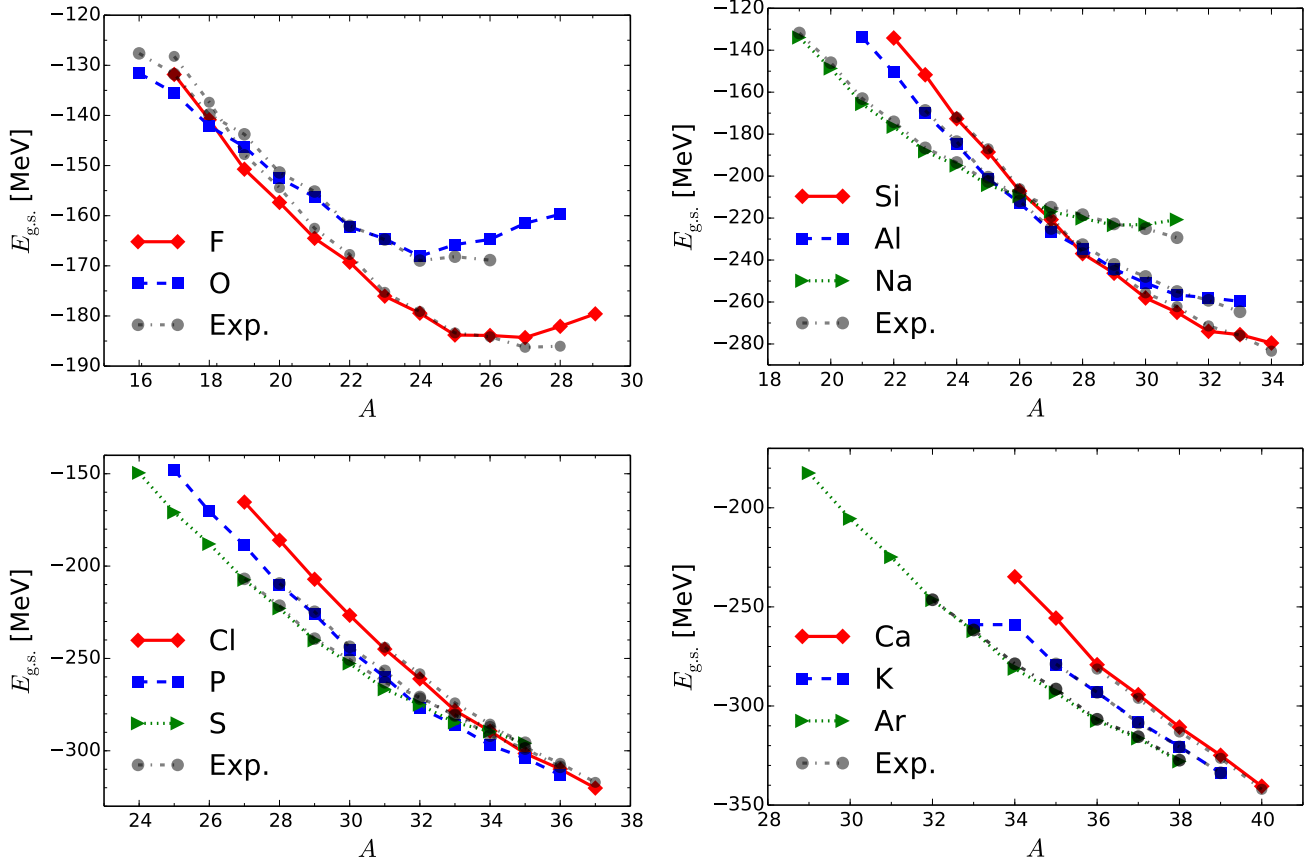


FIG. 4. (Color online) Upper left: Ground-state energies of fluorine (solid line marked with diamonds) and oxygen isotopes (dash-dotted line marked with squares). Upper right: Ground-state energies of silisium (solid line marked with diamonds), aluminium (dash-dotted line marked with squares), and natrium isotopes (dotted line with right triangles). Lower left: Ground-state energies of chlorine (solid line marked with diamonds), phosphorus (dash-dotted line marked with squares), and sulfur isotopes (dotted line with right triangles) Lower right: Ground-state energies of calcium (solid line marked with diamonds), potassium (dash-dotted line marked with squares), and argon isotopes (dotted line with right triangles). Dashed-dotted lines marked with circles show the experimental values. Dashed-dotted lines marked with circles show the experimental values.

a	b	c	d	J	T	$\langle ab H_2^{A_{c+2}} cd\rangle$	a	b	c	d	J	T	$\langle ab H_2^{A_{c+2}} cd\rangle$
2	2	2	2	0	1	-1.209884	1	5	1	5	1	0	-4.732176
2	2	3	3	0	1	-1.267748	1	5	3	6	1	0	-2.634041
2	2	1	1	0	1	-2.813678	1	5	3	4	1	0	1.417620
3	3	3	3	0	1	-0.789697	1	5	1	6	1	0	-1.600826
3	3	1	1	0	1	-0.627860	1	5	1	4	1	0	-0.401344
1	1	1	1	0	1	-0.463086	3	6	3	6	1	0	-2.735304
2	1	2	1	1	1	0.508993	3	6	3	4	1	0	0.063961
2	1	3	1	1	1	-0.145290	3	6	1	6	1	0	-0.004960
3	1	3	1	1	1	0.471263	3	6	1	4	1	0	-0.326177
2	2	2	2	2	1	-0.354285	3	4	3	4	1	0	-4.431654
2	2	2	3	2	1	-0.780041	3	4	1	6	1	0	4.876612
2	2	2	1	2	1	-0.354356	3	4	1	4	1	0	2.230581
2	2	3	1	2	1	-0.752583	1	6	1	6	1	0	-4.488804
2	2	1	1	2	1	-0.604916	1	6	1	4	1	0	-2.255396
2	3	2	3	2	1	-0.540280	1	4	1	4	1	0	-1.443965
2	3	2	1	2	1	-0.200114	2	5	2	5	2	0	-0.748201
2	3	3	1	2	1	-1.191250	2	5	2	6	2	0	-0.726085
2	3	1	1	2	1	-0.394891	2	5	2	4	2	0	-0.272280
2	1	2	1	2	1	0.503484	2	5	3	5	2	0	-0.716467
2	1	3	1	2	1	-0.480941	2	5	1	5	2	0	0.398931
2	1	1	1	2	1	-0.747132	2	5	3	4	2	0	-0.774583
3	1	3	1	2	1	-0.144091	2	5	1	6	2	0	0.667225
3	1	1	1	2	1	-0.240292	2	5	1	4	2	0	-1.247244
1	1	1	1	2	1	0.317194	2	6	2	6	2	0	-1.676750
2	3	2	3	3	1	0.835428	2	6	2	4	2	0	-2.194518
2	3	2	1	3	1	-0.046666	2	6	3	5	2	0	0.132552
2	1	2	1	3	1	0.539996	2	6	1	5	2	0	-2.101734
2	2	2	2	4	1	0.384441	2	6	3	4	2	0	-3.530858
2	2	2	1	4	1	-1.166757	2	6	1	6	2	0	-0.573096
2	1	2	1	4	1	-0.618327	2	6	1	4	2	0	-1.753591
5	5	5	5	0	1	-1.683538	2	4	2	4	2	0	-4.072754
5	5	6	6	0	1	-1.306942	2	4	3	5	2	0	2.186536
5	5	4	4	0	1	-3.025528	2	4	1	5	2	0	-4.432840
6	6	6	6	0	1	-1.176083	2	4	3	4	2	0	-2.600212
6	6	4	4	0	1	-1.100067	2	4	1	6	2	0	-1.389508
4	4	4	4	0	1	-0.774292	2	4	1	4	2	0	-1.303326
5	4	5	4	1	1	0.219121	3	5	3	5	2	0	-1.626130
5	4	6	4	1	1	-0.149186	3	5	1	5	2	0	2.507310
6	4	6	4	1	1	0.225270	3	5	3	4	2	0	0.903296

TABLE II. CCEI two-body matrix-elements for the sd -shell.

a	b	c	d	J	T	$\langle ab H_2^{A_{c+2}} cd\rangle$	a	b	c	d	J	T	$\langle ab H_2^{A_{c+2}} cd\rangle$
5	5	5	5	2	1	-0.788439	3	5	1	6	2	0	2.583444
5	5	5	6	2	1	-0.848394	3	5	1	4	2	0	-2.040815
5	5	5	4	2	1	-0.375108	1	5	1	5	2	0	-4.207750
5	5	6	4	2	1	-0.837176	1	5	3	4	2	0	-1.365998
5	5	4	4	2	1	-0.580298	1	5	1	6	2	0	-2.148594
5	6	5	6	2	1	-0.949096	1	5	1	4	2	0	0.007608
5	6	5	4	2	1	-0.218504	3	4	3	4	2	0	-2.661450
5	6	6	4	2	1	-1.341486	3	4	1	6	2	0	-2.097366
5	6	4	4	2	1	-0.372504	3	4	1	4	2	0	-0.420498
5	4	5	4	2	1	0.191078	1	6	1	6	2	0	-3.186614
5	4	6	4	2	1	-0.552507	1	6	1	4	2	0	1.263075
5	4	4	4	2	1	-0.782881	1	4	1	4	2	0	-0.633272
6	4	6	4	2	1	-0.483819	2	5	2	5	3	0	-1.254326
6	4	4	4	2	1	-0.205074	2	5	2	6	3	0	-1.985546
4	4	4	4	2	1	0.091233	2	5	2	4	3	0	2.550492
5	6	5	6	3	1	0.557494	2	5	3	5	3	0	-2.065423
5	6	5	4	3	1	-0.061753	2	5	1	5	3	0	-2.607278
5	4	5	4	3	1	0.266798	2	5	1	4	3	0	-0.091707
5	5	5	5	4	1	0.017251	2	6	2	6	3	0	-3.719068
5	5	5	4	4	1	-1.289670	2	6	2	4	3	0	1.264112
5	4	5	4	4	1	-1.041445	2	6	3	5	3	0	-4.705594
2	5	2	5	0	0	-1.835201	2	6	1	5	3	0	-1.304042
2	5	3	6	0	0	-1.311656	2	6	1	4	3	0	-0.163411
2	5	1	4	0	0	-3.023355	2	4	2	4	3	0	2.816222
3	6	3	6	0	0	-1.209983	2	4	3	5	3	0	0.595824
3	6	1	4	0	0	-1.087112	2	4	1	5	3	0	-3.405766
1	4	1	4	0	0	-0.929649	2	4	1	4	3	0	-0.304057
2	5	2	5	1	0	-1.895294	3	5	3	5	3	0	-3.428880
2	5	2	4	1	0	3.680259	3	5	1	5	3	0	-0.117532
2	5	1	5	1	0	-3.479575	3	5	1	4	3	0	0.732445
2	5	3	6	1	0	-1.103603	1	5	1	5	3	0	5.259282
2	5	3	4	1	0	-0.124722	1	5	1	4	3	0	0.951971
2	5	1	6	1	0	0.148509	1	4	1	4	3	0	-1.947045
2	5	1	4	1	0	1.543712	2	5	2	5	4	0	-0.014895
2	4	2	4	1	0	-5.374974	2	5	2	4	4	0	-1.281840
2	4	1	5	1	0	5.491716	2	5	1	5	4	0	1.246601
2	4	3	6	1	0	2.778464	2	4	2	4	4	0	-5.746248
2	4	3	4	1	0	-1.876604	2	4	1	5	4	0	-3.402626
2	4	1	6	1	0	1.515858	1	5	1	5	4	0	-5.378448
2	4	1	4	1	0	0.373965	2	5	2	5	5	0	-4.184793

TABLE III. CCEI two-body matrix-elements for the sd -shell.